Anal Bioanal Chem
DOI 10.1007/s00216-017-0416-5

RESEARCH PAPER

Design of a novel electrochemical biosensor based on intramolecular G-quadruplex DNA for selective determination of lead(II) ions

Maryam Ebrahimi[1] · **Jahan Bakhsh Raoof**[1] · **Reza Ojani**[1]

Received: 14 January 2017 / Revised: 14 April 2017 / Accepted: 15 May 2017

Abstract An electrochemical DNA biosensor based on a G-quadruplex (G4) for the sensitive determination of Pb^{2+} was reported using a carbon paste electrode (CPE) or a multi-walled carbon nanotube paste electrode (MWCNTPE) as working electrodes, ethyl green (EG) as a new G4 intercalator, and a single-stranded nucleic acid sequence rich in guanine (G) as DNA probe. Electrochemical determination of Pb^{2+} relied on probe structural changes from single - stranded to the stabilized intramolecular G4 in the presence of Pb^{2+}, which caused a change in the current of the EG reduction peak due to the intercalation of EG into the G4 structure. The change in the reduction peak of EG before and after its intercalation into the stabilized G4 (ΔI) had a linear correlation to the concentration of Pb^{2+} ions. The linear ranges of 4.0×10^{-10}–5.0×10^{-9} M and 2×10^{-7}–1×1^{-5} M with a detection limit (LOD) of 1.04×10^{-10} M were obtained using CPE, while improved linear ranges of 4.0×10^{-11}–1.0×10^{-9} M and 2×10^{-7}–1×10^{-5} M with a lower LOD of 2.64×10^{-11} M were achieved using the MWCNTPE biosensor. The biosensors exhibited satisfactory results in terms of selectivity and practical applicability in the analysis of real samples.

Keywords Lead ion · Intramolecular G-quadruplex · Carbon nanotubes · Ethyl green · DNA biosensor

✉ Jahan Bakhsh Raoof
j.raoof@umz.ac.ir

[1] Eletroanalytical Chemistry Research Laboratory, Department of Analytical Chemistry, Faculty of Chemistry, University of Mazandaran, Babolsar, Mazandaran 47416-1467, Iran

Introduction

Lead ions, as one of the most hazardous heavy metal ions, have adverse effects on the environment and human health because of their toxic nature [1–3]. The accumulation of these ions in the human body can result in several diseases such as the renal and nervous system damages [3–5]. On the other hand, lead is one of the most abundant natural substances [6] which has been used in many industries, including smelting, mining, refining, battery manufacturing, and so on [7]. Thus, widespread existence of lead in the environment is of the major public health concerns [8, 9]. Therefore, the selective and sensitive monitoring of Pb^{2+} in the environmental and biological samples is very important [3, 4, 10]. The majority of classical methods for Pb^{2+} ion detection such as inductively coupled plasma mass spectrometry (ICP-MS) [11, 12], atomic absorbance spectrometry (AAS) [13, 14], NMR [15], fluorescent [16, 17], and colorimetric [18, 19] suffer from expensive equipments and laborious pre-treatment processes [3, 20]. Electrochemical methods have overcome these limitations due to their excellent properties, such as high selectivity, low cost, short measuring period, and simple procedures [3, 21, 22].

In recent years, detection of metal ions through their affinity for nucleic acids has attracted considerable attention and several nucleic acid-based sensors for electrochemical determination of heavy metal ions have been developed [23–25]. As an important type of these sensors, up to now, a few electrochemical G-quadruplex DNA (G4) sensors as one important type of these sensors are reported for determination of metal ions especially lead ions [1–4, 26]. G4 is one of the nucleic acid secondary structures formed from guanine-rich sequences which are capable of forming a four-stranded structure around guanine tetrads (G-tetrads) [27–30]. This structure

Published online: 07 June 2017

is stabilized in the presence of some cations such as K^+, Na^+, Pb^{2+}, etc. [27–30]. Interaction of these cations within eight guanines in two adjacent G-tetrads can cause G-rich DNA conformational change from a single-stranded DNA (ssDNA) structure to stabilized G4 [27–30]. Some small electroactive molecules, owing to their intercalation into the G4, can act as G4-binding label [4, 25]. Moreover, their electrochemical signal can be applied for the detection of metal ions [4, 25, 26]. Accordingly, two dyes from triphenylmethane family, i.e., crystal violet (CVi) and malachite green (MG), due to their binding to G4 were used as sensitive G4 biosensors [31, 32] and a sensitive G4 biosensor based on electrochemical signal of CVi has been developed for sensitive Pb^{2+} sensing [4].

Immobilization of nucleic acid probes on the electrode surface is a key step in development of electrochemical nucleic acid biosensors, which has significant effect on the performance of biosensors [33–35]. Several strategies have been reported for probe immobilization on electrode surfaces, such as electrochemical adsorption [23, 24, 36, 37], physical adsorption [38, 39], covalent bonding [1–4, 40, 41], probe entrapment [42, 43], and biotin-avidin complexation [35, 44]. Among them, covalent bonding of probes on carbonaceous electrodes by modification of electrodes with amino or carboxyl group [45, 46] and on gold electrodes via self-assembly of hydroxyl-, carboxyl-, or amino-modified sulfur-containing compounds [40] or direct self-assembly of thiol-functionalized DNA probe on electrode surfaces [1–4, 41] are very common. However, this method requires costly, tedious, and time-consuming prior modification/treatment of DNA and/or electrode surface [33, 47], while adsorption procedure is the simplest method to immobilize the probe on electrode because it does not require these time-consuming and expensive pre-treatments [47, 48]. Carbonaceous electrodes are very suitable electrodes for adsorption immobilization of probe because of their chemical and physical properties such as porosity and high internal surface area [47]. To the best of our knowledge, a few electrochemical G4-based sensors have been developed for determination of lead ions, and in all of them, covalent attachment has been used for immobilization of probe on gold electrodes [1–4].

In this work, we adopted carbon paste electrode (CPE) as working electrode not only to gain advantageous properties of CPE such as easy and very low-cost preparation, renewability, low ohmic resistance [49], wide potential window, and low background current [47] but also to save the time and cost by applying electrochemical adsorption as the most effective and the easiest technique for DNA immobilization on CPE [47] performed by applying a positive potential to the electrode [35, 47]. Furthermore, we could improve electrochemical performance of designed sensor by modification of CPE with MWCNT due to the ultrahigh surface area of CNT, leading to an enhancement in probe immobilization and consequently a lower detection limit [50]. Ethyl green (EG) is a triphenylmethane dye which has not only a similar structure to CVi and MG but also two positive charges in its structure that can help interaction with the negatively charged G4 (Scheme 1a). Hence, we investigated the interaction mode of EG–G4 and the ability of EG as G4 intercalator to detect lead ions. The stabilized G4 formation was studied by circular dichroism (CD) measurements, and interaction mode between G4 and EG was identified by UV–vis spectroscopy and differential pulse voltammetry (DPV) techniques. DPV was also used for electrochemical measurements of lead ions. In addition, the selectivity of these biosensors for voltammetric determination of Pb^{2+} against other heavy metal ions and the practical utility of the biosensors for real sample analysis were evaluated.

Experimental

Materials and reagents

The oligonucleotide (5′-GGGT GGGT GGGT GGGT-3′) as the probe was synthesized by MWG-BIOTECH (Germany). Sodium chloride, potassium chloride, and silver (I) nitrate were purchased from Merck Company. Mercuric chloride, lead(II) nitrate, EG, potassium ferricyanide, and potassium ferrocyanide were supplied from Fluka. The stock solution of DNA (1.0 μM) was prepared with 50 mM Tris buffer (50 mM Tris-HCl, 1.0 mM EDTA, pH 8.00), followed by storing in the freezer. For preparation of double-stranded DNA (dsDNA), the solution containing ssDNA and its complementary DNA was heated in a water bath at 100 °C for 10 min and allowed to cool at room temperature. Stock solutions of 1.0 mM metal ions were prepared in 50.0 mM Tris–HCl buffer (pH 7.40) supporting electrolyte. EG solution was prepared under the same condition as that of used for metal solution preparation. We used the distilled, deionized, and sterilized water in all solution preparation.

Apparatus

AUTOLAB PGSTAT 30 electrochemical analysis system and GPES 4.9 software package and FRA software (Eco Chemie, The Netherlands) were applied for electrochemical measurements in three electrode system including a bare CPE or MWCNTPE as working electrode, a platinum wire as the auxiliary electrode, and a saturated calomel electrode (SCE) as the reference electrode. A computing double beam UV spectrophotometer (CECIL 5000, Elegant Technology) and 1.0-cm quartz cells were used for spectrophotometric measurements. CD measurements were conducted by a Model 215 CD recorder (Aviv, USA) from 320 to 200 nm using 1-cm path-length standard quartz cells. A Hitachi S-1460 field emission scanning electron microscope using an AC voltage of 15 kV was utilized to obtain field emission scanning electron microscopy (FE-SEM) images. The pH measurements were performed using an Ion Analyzer 250 Corning pH meter.

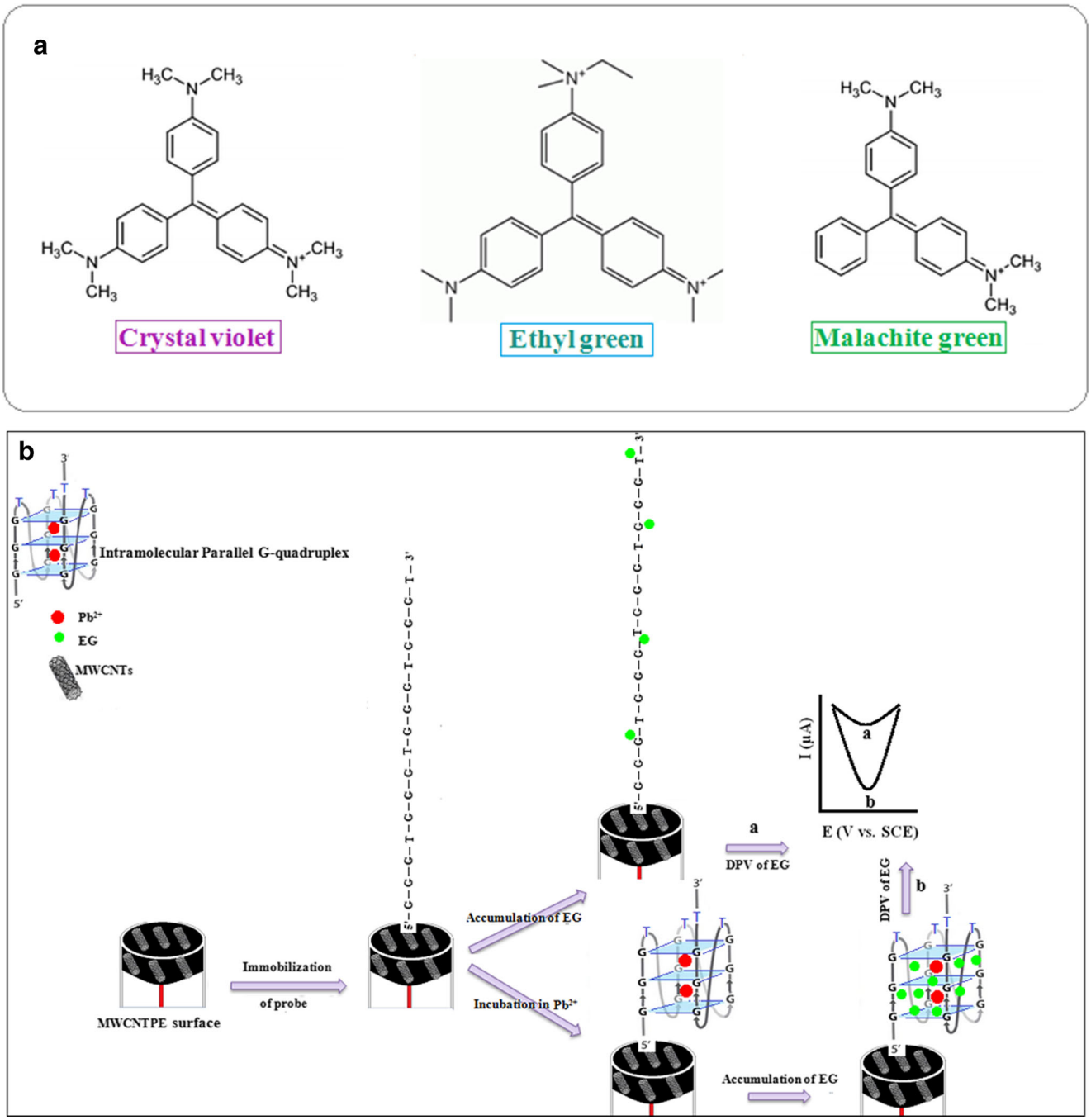

Scheme 1 Structures of three triphenylmethane dyes: Malachite green, Crystal violet, and Ethyl green (**A**) and the principle of the electrochemical sensing of Pb^{2+} based on intramolecular G-quadruplex using EG (**B**)

Procedure

Probe-modified electrode preparation

The carbon paste electrode was prepared according to the method reported in our previous works [23, 24]. For preparation of MWCNTPE, graphite powder, paraffin oil, and MWCNT were thoroughly mixed in a ratio of 60:33:7% (*w*/*w*) [51]. Subsequent steps of preparation of this electrode were similar to preparation of CPE.

The electrochemical adsorption technique was adopted for immobilization of the probe on the working electrodes performed by applying a positive potential to electrode surfaces. The positively charged carbon surfaces lead to their strong electrostatic interaction with DNA as polyanionic molecule, resulting in significant improvement in the stability and mechanical resistance of electrode [35, 47]. Considering the oxidation potential of adenine and guanine as the electroactive bases of DNA, i.e., 1.1 and 0.8 V, vs. SCE, respectively [47], the applied potential should be lower than these values [47]. Electrochemical adsorption of

probe on carbonaceous electrodes is increased by anodic pretreatment of electrode surface through increasing the density of surface oxygenated groups and hydrophilic property of surface and elimination of surface contaminants, resulting in enhanced adsorption [35, 47]. Therefore, the prior electrode surface activation before the adsorption immobilization is necessary [35]. We activated the surface of CPE or MWCNTPE electrochemically under optimized potential (1.80 V vs. SCE) [23, 24] in 0.50 M acetate buffer solution (pH 4.8) containing 20 mM NaCl without stirring for 5 min. Subsequently, the immobilization of 10^{-6} M probe on the activated electrode was carried out by applying a potential of 0.50 V vs. SCE to the electrodes for 5 min under stirring followed by thorough rinsing the electrodes with sterilized and deionized water.

Pb^{2+}-induced G4 DNA formation

The G4 was formed by incubating the probe-modified CPE or MWCNTPE in the stirring Pb^{2+} solution (0.5 M Tris–HCl buffer solution, pH 7.40) containing different concentrations of Pb^{2+} for 5 min (the optimum time, data not shown) without applying any potential to the electrode. The electrode was then rinsed with sterilized and deionized water. Selectivity test of biosensor was conducted by the same procedure.

Intercalating of EG in formed G4

The accumulation of label was done on the probe-modified electrodes by incubating the electrode in 50 mM Tris–HCl buffer solution (pH 7.4) containing 1.0 mM EG for 5 min (the optimum time, data not shown), followed by rinsing with sterilized and deionized water. Solution or electrode was not stirred, and any potential was not applied to the electrode.

Voltammetric determination of Pb^{2+}

The electrochemical determination of Pb^{2+} was carried out by DPV measurements of reduction peak current of EG in Tris–HCl buffer solution with cathodic potential scan from 0.7 to 0.2 V vs. SCE at the modulation amplitude of 0.04995 and step potential of 0.01005 V vs. SCE.

Results and discussion

Characterization of MWCNTs

Figure 1 shows FE-SEM images of carbon paste (A), multi-walled carbon nanotubes (B), and multi-walled carbon nanotubes paste (C). As can be seen, the diameter range of carbon nanotubes was 17–23 nm.

Investigation of working electrode surfaces

Figure 2a, b shows the cyclic voltammograms and the Nyquist plots of 1.0 mM $K_3[Fe(CN)_6]/K_4[(CN)_6]$ at the bare CPE and MWCNTPE, respectively. An increase in the voltammetric peak current and the decrease in the peak separation of $Fe(CN)_6^{3-/4-}$ at the surface of MWCNTPE compared to that of obtained at the surface of CPE (Fig. 2a) confirmed the increased conductivity of the modified electrode. The electron transfer resistance, R_{ct}, of $Fe(CN)_6^{3-/4-}$ redox couple at the MWCNTPE surface (R_{ct} = 244 Ω) was significantly lower than CPE (R_{ct} = 451 Ω; Fig. 2b) which shows that the presence of CNTs resulted to an improvement in surface properties of the CPE and a decrease in the electron transfer resistance.

Demonstration of Pb^{2+}-induced G-quadruplex formation

G-quadruplexes can be classified based on the numbers of DNA strands involved in its formation as intramolecular (a single strand), bimolecular (two strands), and tetramolecular (four strands) [28, 29] and based on the orientation and arrangement of strands as the parallel-stranded structure and the antiparallel-stranded structure [27–30]. CD spectroscopy is an efficient technique for the study of conformations of nucleic acids and proteins based on the difference in absorbance of a substance in right- and left-handed orientation with circularly polarized light [52, 53]. CD spectroscopy can distinguish the parallel and antiparallel G4 structures. CD spectrum of parallel-stranded G4 displays a maximum at ~260 nm and a minimum at ~240 nm, while the CD maximum and minimum of antiparallel-stranded G4 are observed at ~290 and 260 nm, respectively [27]. The spectrum in Fig. 3 revealed that in the presence of Pb^{2+}, the probe formed a parallel G-quadruplex (curve a). In the presence of EG, CD spectrum did not show significant change (curve b), indicating EG cannot noticeably affect the G4 structures and Pb^{2+} ions are responsible for the formation and the stabilization of G4. These results are very similar to those obtained from investigation of CVi dye as G-quadruplex intercalator [4]. Curve c indicates that height of the maximum and minimum peak at CD spectrum increased after giving 5 min time for interaction between DNA probe and Pb^{2+}.

EG as a DNA G4 intercalator

G4–EG interaction mode was investigated by spectroscopic and voltammetric studies. Generally, small molecules can bind to DNA via three dominant noncovalent modes, i.e., electrostatic binding, intercalation binding, and groove binding [54, 55]. The electrochemical and spectroscopic results of our previous work indicated that the EG interaction mode with ssDNA or dsDNA is partly intercalation and their domain

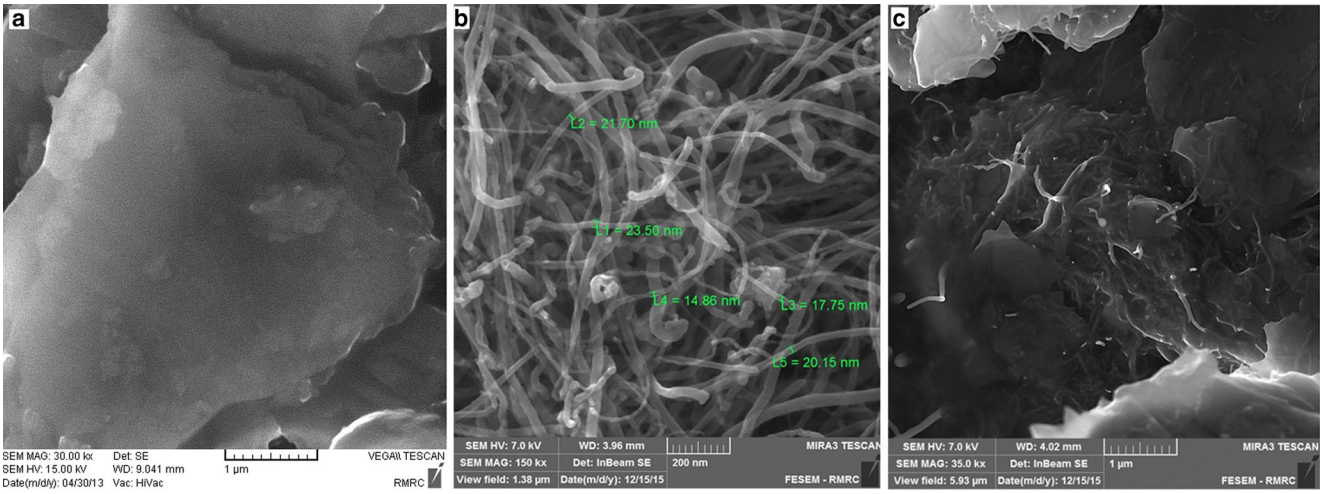

Fig. 1 FE-SEM images of carbon paste (**A**), multi-walled carbon nanotubes (**B**), and multi-walled carbon nanotubes paste (**C**)

interaction mode is electrostatic [23, 24]. In this paper, the interaction mode between G4 and EG was studied.

Absorption spectroscopic study

The useful information concerning the mode and intensity of small molecules-DNA binding can be achieved from the results of spectroscopic studies [56]. Figure 4 shows the UV-Vis spectra of EG before (curve a) and after adding ssDNA (probe) (curve b), dsDNA (curve c), and different amounts of G4 (probe + different concentrations of Pb^{2+}) (curves d–g). As can be seen, after mixing EG with ssDNA and dsDNA, the absorption maximum of the EG shifts from 630.4 nm to 631.6 and 633.0 nm and the absorbance decreases from 0.0912 to

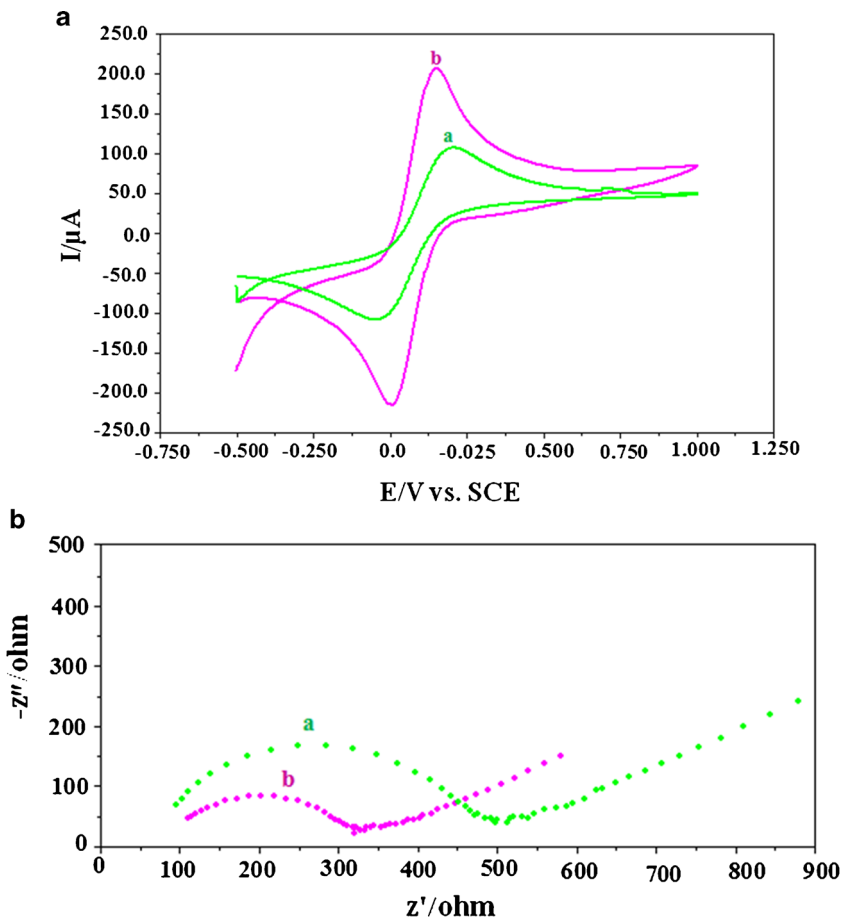

Fig. 2 CV curves (**A**) and Nyquist plots (**B**) of 1.0 mM $K_3[Fe(CN)_6]$ / 1.0 mM $K_4[Fe(CN)_6]$ in 10 mM Tris-HCl buffer solution (pH 7.0) at (**a**) bare CPE and (**b**) MWCNTPE. CV scan rate 100 mV s^{-1}

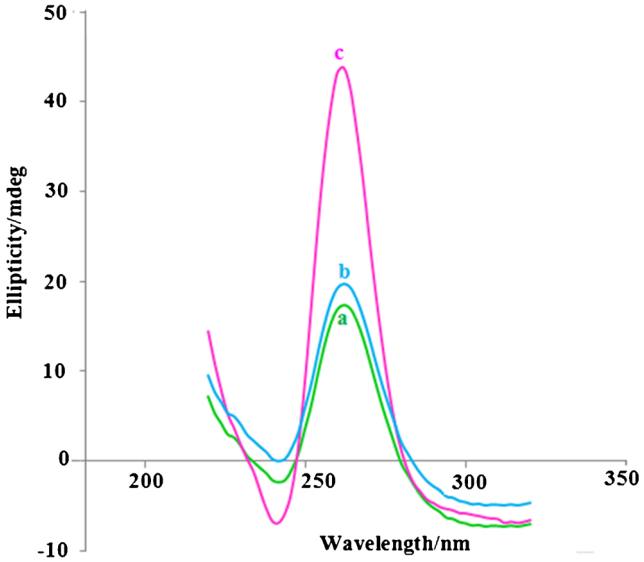

Fig. 3 CD spectra of Pb^{2+}-probe (**a**), Pb^{2+}-probe in the presence of EG (**b**), and Pb^{2+}-probe after 5 min interaction (**c**)

0.0875 and 0.0846, respectively. However, these changes in absorption spectrum of EG are significant in the presence of G-quadruplex. Intercalation of DNA with low molecular weight compound usually leads to a shift of the maximum absorbance to higher wave lengths (red shift effect or bathochromic effect) and decreasing in absorbance

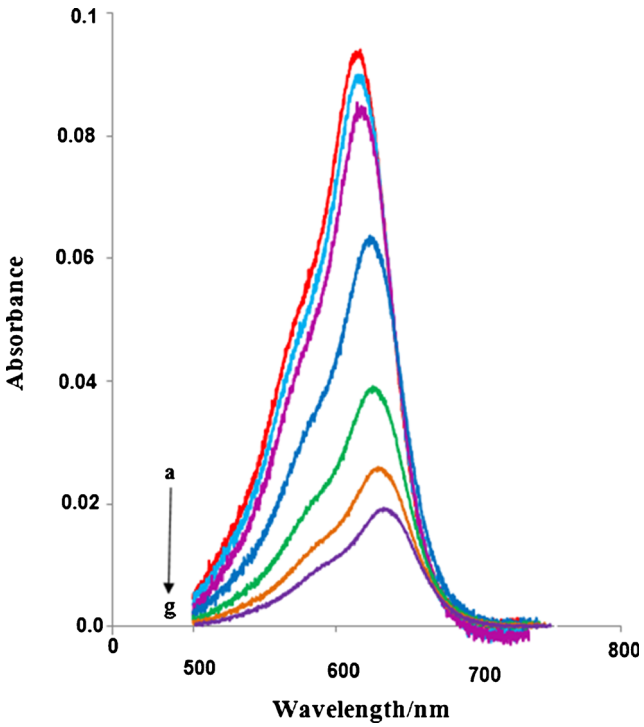

Fig. 4 The UV-Vis spectra of 10^{-5} M EG (curve a), ssDNA-EG (curve b), dsDNA-EG (curve c), G4 (probe in the presence of 10^{-6} M Pb^{2+})-EG (curve d), G4 (probe in the presence of 10^{-5} M Pb^{2+})-EG (curve e), G4 (probe in the presence of 10^{-4} M Pb^{2+})-EG (curve f), and G4 (probe in the presence of 10^{-3} M Pb^{2+})-EG (curve g)

(hypochromism effect) [57, 58]. However, red shift and hypochromism effects observed in EG-ssDNA and EG-dsDNA (4.0% and 1.2 nm for EG-ssDNA and 7.2% and 2.6 nm for EG-dsDNA) are not noticeable compared with those observed in typical classical intercalators [59, 60], while these values for EG–G4 (32.56%, 10.4 nm) are large enough to prove the intercalating of EG into G4 (curves d). As can be seen, these values increased with increasing the amounts of G4 owing to the increasing of Pb^{2+} concentrations (curves e–g).

Voltammetric study in solution

Electrochemical study has been used in DNA-small molecules interaction investigation [54, 55]. Based on the report of Bard et al. [61], positive peak potential shift of molecule in voltammetric measurements indicates intercalation interaction of molecule with DNA, while electrostatic interaction leads to negative shift of potential. Figure 5 shows the differential

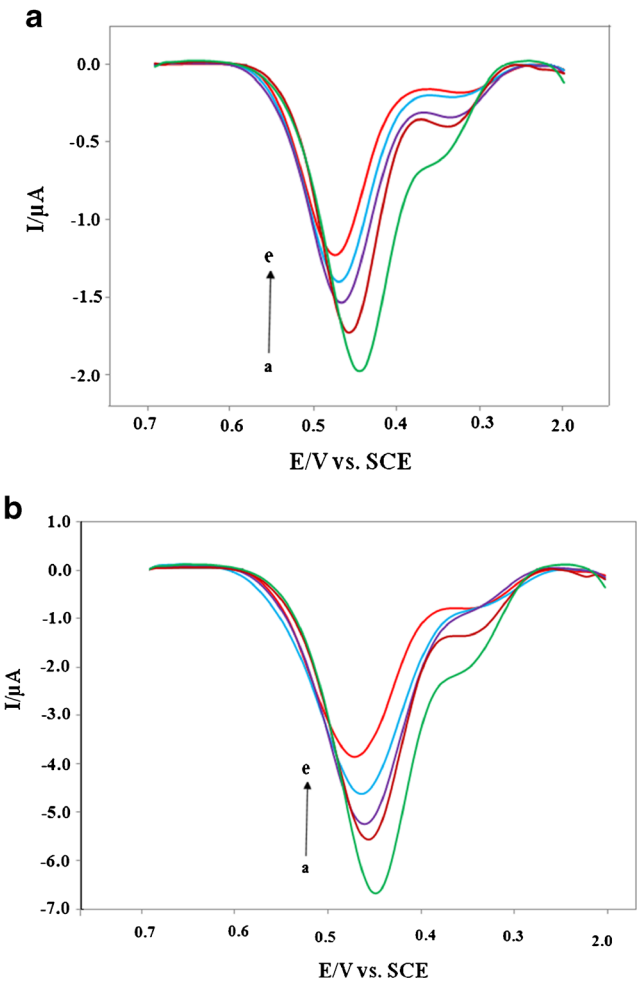

Fig. 5 DPV response curves of 10^{-5} M EG in solution before (curve a) and after adding probe + different concentrations of Pb^{2+}: 10^{-6} M Pb^{2+} (curve b), 10^{-5} M (curve c), 10^{-4} M (curve d) and 10^{-3} M (curve e) at (**A**) CPE and (**B**) MWCNTPE

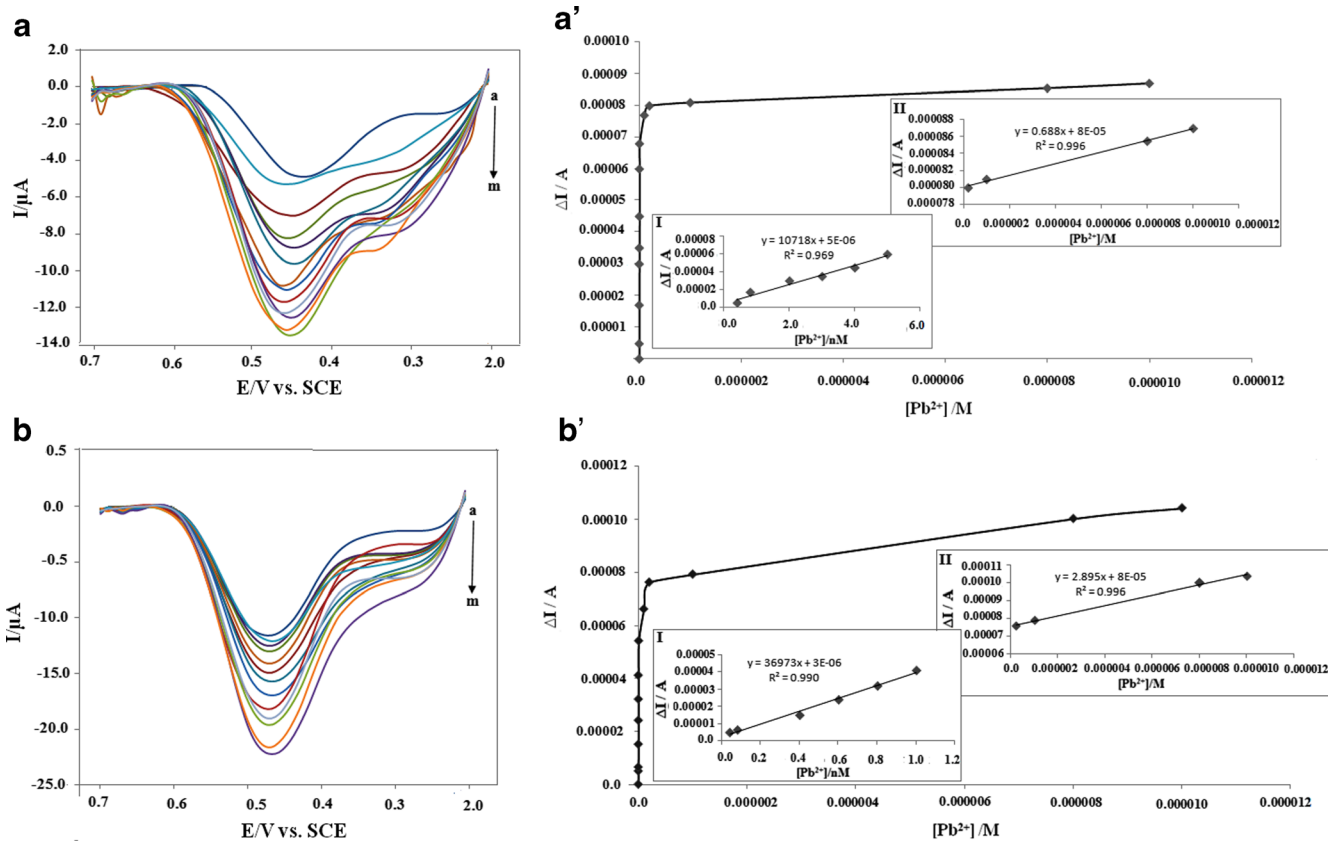

Fig. 6 DPV signals of 10^{-3} M accumulated EG on the probe-immobilized working electrode after incubation in different concentrations of lead ions including (**A**) (a) 0.0, (b) 0.4, (c) 0.8, (d) 2.0, (e) 3.0, (f) 4.0, (g) 5.0, (h) 6.0, (i) 1×10^2, (j) 2×10^2, (k) 1×10^3, (l) 8×10^3, and (m) 1×10^4 nM in 50 mM Tris–HCl buffer solution (pH 7.4) at CPE and (**B**) (a) 0.00, (b) 0.04, (c) 0.08, (d) 0.4, (e) 0.6, (f) 0.8, (g) 1.0, (h) 6.0, (i) 1×10^2, (j) 2×10^2, (j) 1×10^3, (l) 8×10^3, and (m) 1×10^4 nM in 50 mM Tris–HCl buffer solution (pH 7.4) at MWCNTPE. The difference of DPV responses against the lead ion concentrations at (**A'**) CPE: the *inset* shows the related calibration plot of Pb^{2+} concentration over the range (I) 0.4–5.00 nM and (II) 0.2–10.0 μM and (**B'**) MWCNTPE. The *inset* shows the related calibration plot of Pb^{2+} concentration over the range 0.04–1.00 nM and (II) 0.2–10.0 μM

pulse voltammograms of EG before (curve a) and after adding different amounts of G4 (curves b–e). As can be seen, the reduction peak currents of EG after adding G4 at the surface of CPE and MWCNTPE decreased about 1.1 and 0.13 μA, respectively, and reduction peak potentials of EG shifted positively about 10 and 20 mV, respectively (curve b). In addition, these values increased gradually with increasing amounts of G4 owing to the increasing Pb^{2+} concentrations (curves c–e).

Table 1 Comparison of the G4-based biosensors for the electrochemical detection of lead ions

Electrode	Probe	Immobilization method	Determination technique	LOD	Linear range	Reference
Gold electrode	5′-HO-$(CH2)_6$-SS-$(CH2)_6$TTTTTCCAACGGTTGGTGTG GTTGG-3′	Covalent binding	EIS	0.5 nM	0.5 nM– 50 μM	[1]
Gold electrode	TBA:5′-SH-$(CH2)_6$- GGT TGG TGT GGT TGG-3′	Covalent binding	DPV	4.2 nM	5.0 nM– 10 μM	[2]
Gold electrode	TBA:5′-SH-$(CH2)_6$- GGT TGG TGT GGT TGG-3′	Covalent binding	SWV	34.7 nM	0.05–1.0 μM	[3]
Gold electrode	5′-SH -$(GGGT)_4$-3′	Covalent binding	DPV	0.4 nM	1.0 nM–1.0 μM	[4]
MWCNTPE	5′-$(GGGT)_4$-3′	Electrochemical adsorption	DPV	26.4 pM	40 pM–1.0 nM 0.2–10.0 μM	This paper
CPE	5′-$(GGGT)_4$-3′	Electrochemical adsorption	DPV	0.1 nM	0.4–5.0 nM 0.2–10.0 μM	This paper

SWV square wave voltammetry

Table 2 Real analysis of Pb^{2+} in water samples

Water sample	Pb^{2+} added /M	Pb^{2+} found /M [a]	Recovery (%)	Electrode
Tap water [b]	0.0	Not detectable	–	CPE biosensor
	0.0	Not detectable	–	CNTPE biosensor
	1.0×10^{-9}	$0.92\ (\pm 0.03) \times 10^{-9}$	92.0	CPE biosensor
	1.0×10^{-9}	$0.97(\pm 0.02) \times 10^{-9}$	97.0	CNTPE biosensor
	1.0×10^{-6}	$0.90(\pm 0.\ 05) \times 10^{-6}$	90.0	CPE biosensor
	1.0×10^{-6}	$1.08(\pm 0.\ 08) \times 10^{-6}$	108.0	CNTPE biosensor
Sea water [c]	0.0	$0.62(\pm 0.05) \times 10^{-9}$	–	CPE biosensor
	0.0	$0.53(\pm 0.04) \times 10^{-9}$	–	CNTPE biosensor
	1.0×10^{-9}	$1.51(\pm 0.03) \times 10^{-9}$	93.2	CPE biosensor
	1.0×10^{-9}	$1.59(\pm 0.01) \times 10^{-9}$	103.9	CNTPE biosensor
	1.0×10^{-6}	$0.93\ (\pm 0.06) \times 10^{-6}$	92.94	CPE biosensor
	1.0×10^{-6}	$0.95(\pm 0.04) \times 10^{-6}$	94.95	CNTPE biosensor

[a] Mean value ± SD (standard deviation), $n = 5$

[b] From drinking water system of Babolsar, Iran

[c] From Caspian Sea, Babolsar, Iran

These changes indicated that EG intercalated into G4, which was consistent with the result of absorption measurements.

Electrochemical determination of Pb^{2+} at G4 biosensor via differential pulse voltammograms

The differential pulse voltammograms of 10^{-3} M EG intercalated into G4 in the presence of 10^{-5} M Pb^{2+} were recorded for determination of Pb^{2+}. Intercalation of EG in formed G4 due to the probe structural switching from ssDNA to Pb^{2+}-stabilized G4 in the presence of Pb^{2+} led to the increase in the DPV peak current of EG accumulated on the electrode. DPV peak currents of 10^{-3} M EG accumulated on the probe-modified electrode at the surface of CPE and MWCNTPE are displayed in Fig. 6a, b Curve a, respectively, and DPV signals of 10^{-3} M EG accumulated on the probe-modified electrode in a stirred Pb^{2+} solution (0.5 M Tris–HCl buffer solution, pH 7.40 containing 10^{-5} M Pb^{2+}) were shown in curve k (Fig. 6a, b). As can be seen, the peak current of EG after intercalating of EG in the formed G4 increased due to the presence of lead ions. When probe-modified electrode was not incubated in Pb^{2+} solution, the probe cannot form a stabilized G4, while when this electrode was incubated in a certain amount of Pb^{2+} solution, the peak current of EG on the electrode increased significantly because of intercalation of EG into G4. We used the difference in the value of the peak currents of EG before and after its intercalation into the stabilized G4 (ΔI) for electrochemical determination of lead ions since the increased peak currents of EG were proportional to the Pb^{2+} concentrations. Scheme 1b illustrates the principle of the electrochemical sensing of lead ions based on intramolecular G-quadruplex using EG.

DPV was applied for investigating the reduction signals of accumulated EG on both working electrodes due to the formation of different stabilized G-quadruplexes in the presence of different concentrations of Pb^{2+}. Figure 6a, b shows

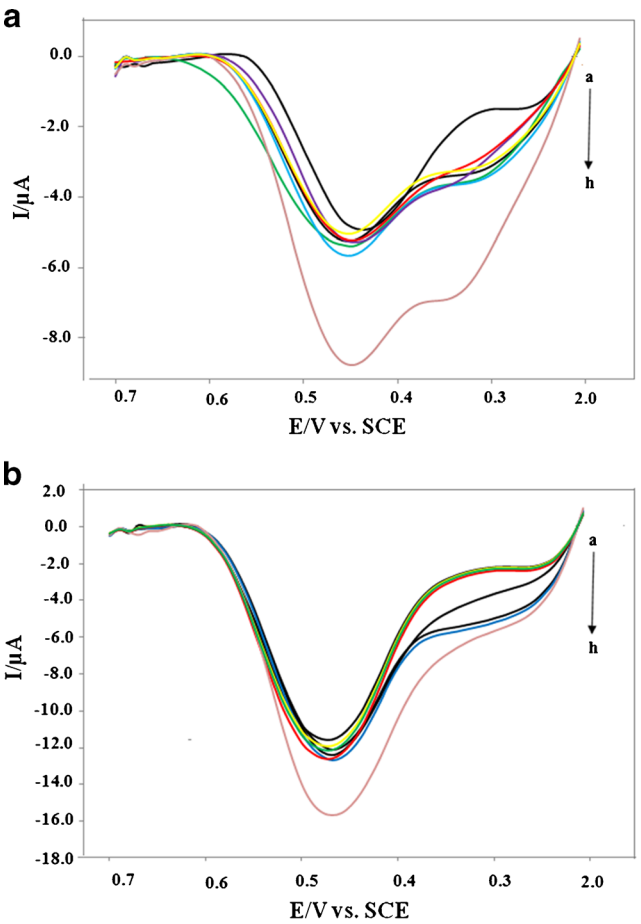

Fig. 7 DPV response curves of 10^{-3} M accumulated EG at probe-modified working electrode (a) before and after incubation in 1.0 μM (b) Ca^{2+}, (c) Cd^{2+}, (d) Na^{+}, (e) K^{+}, (f) Hg^{2+}, (g) Ag^{+}, and 0.1 μM (g) Pb^{2+} at (**A**) CPE and (**B**) MWCNTPE

the linear correlation of ΔI of 10^{-3} M EG to the concentration of Pb^{2+} over the ranges 4.0×10^{-10}–5.0×10^{-9} M and 2.0×10^{-7}–1.0×10^{-5} M for biosensor and 4.0×10^{-11}–1.0×10^{-9} M and 2.0×10^{-7}–1.0×10^{-5} M for MWCNT-modified biosensor, respectively. As can be seen, in both electrodes, the electrochemical signal of EG and subsequently ΔI increased clearly with increasing the amount of the Pb^{2+}. The detection limits were calculated 1.04×10^{-10} and 2.64×10^{-11} M based on a signal-to-noise ratio of three for biosensor and MWCNT-modified biosensor, respectively. As expected, the electrochemical performance of G4-based biosensor was improved, owing to the presence of MWCNTs in the carbon paste.

Selectivity study for Pb^{2+} detection at G4 biosensor

The selectivity of the biosensor was evaluated by using several metal ions including Ca^{2+}, Ag^{+}, K^{+}, Hg^{2+}, Cd^{2+}, and Na^{+}. Figure 6 shows the enhanced DPV peak of EG at the probe-modified electrode incubated in 1.0 nM Pb^{2+} and other competing metal ions with 1.0 μM concentration using DPV measurements. As can be seen, these metal ions have insignificant effect on the detection of Pb^{2+} in both biosensors. These results demonstrated a satisfactory selectivity of the proposed electrochemical biosensors for Pb^{2+} determination.

We compared some similar electrochemical G4-based sensors for lead ion determination (Table 1). According to LOD of both proposed biosensors in this work, the result of this comparison was promising. Nevertheless, the practical utility of the biosensor should be evaluated.

Voltammetric determination of Pb^{2+} in real sample at G4 biosensor

Recovery experiments using spiked water samples were carried out to demonstrate the practical application of the proposed sensors in lead ions determination. Both tap and sea water samples spiked with 0.0 and 1.0 nM and 1.0 μM of Pb^{2+}, and as can be seen in Table 2, the satisfactory recovery values of spiked Pb^{2+} in water samples indicated the ability of the proposed approach for the detection of Pb^{2+} in real samples in both low and high level of concentrations.

Stability and reproducibility of G4-based biosensor

We have also evaluated the stability and reproducibility of biosensor. DPV peak currents of EG intercalated into G4 in the presence of 1.0 nM Pb^{2+} on the surface of eight probe-modified CPEs and CNTPEs were applied to investigate reproducibility of the sensor. The relative standard deviations (RSDs) of peak currents obtained 7.5 and 6.5% for CPE and MWCPE, respectively. In addition, the reproducibility of the sensor was evaluated by recording DPV signals of EG on one electrode for eight times with the RSDs of 6.5 and 5.5% for CPE and MWCPE, respectively. The stability of sensor was also investigated by DPV responses of EG on the probe-modified electrode surfaces which were stored for 2 weeks at 4 °C. DPV responses of EG on CPE and MWCPE surfaces lost only 8 and 6% of their initial values, respectively. These results indicated the proposed sensor had satisfactory stability and reproducibility (Fig. 7).

Conclusion

In this work, the electrochemical DNA biosensors for the determination of lead ions were designed. The ssDNA probe formed intramolecular parallel G4 structure in the presence of Pb^{2+} and subsequent intercalating of EG in formed G4 led to the significant increase in the peak currents of EG as an electroactive label. The difference in the value of peak currents of label before and after its intercalation into the stabilized G4 (ΔI) was applied for selective and sensitive electrochemical determination of lead ions. Both biosensors showed satisfactory analytical performance for Pb^{2+} determination in comparison to other developed sensors.

Compliance with ethical standards

Conflict of interest The authors declare that they have no conflict of interest.

Human and animal rights This work does not contain any studies with human participants or animals.

References

1. Lin Z, Chen Y, Xi L, Fang W. Pb^{2+} induced DNA conformational switch from hairpin to G-quadruplex: electrochemical detection of Pb^{2+}. Analyst. 2011;136:2367–72.
2. Bala A, Pietrzak M, G'orski Ł, Malinowska E. Electrochemical determination of lead ion with DNA oligonucleotide-based biosensor using anionic redox marker. Electrochim Acta. 2015;180:763–9.
3. Jarczewska M, Kierzkowska E, Zilkowski R, G'orski Ł, Malinowska E. Electrochemical oligonucleotide-based biosensor for the determination of lead ion. Bioelectrochemistry. 2015;101:35–41.
4. Li F, Feng Y, Zhao C, Tang B. Crystal violet as a G-quadruplex-selective probe for sensitive amperometric sensing of lead. Chem Commun. 2011;47:11909–11.
5. Yang C, Liu L, Zeng T, Yang D, Yao Z, Zhao Y, et al. Highly sensitive simultaneous detection of lead(II) and barium(II) with G-quadruplex DNA in α-hemolysin nanopore. Anal Chem. 2013;85:7302–7.
6. Abdollahi M, Sadeghi Mojarad A, Jalali N. Lead toxicity in employees of a paint factory. MJIRI. 1996;10:203–6.
7. Mohammadi S, Mehrparvar A, Aghilinejad M. Appendectomy due to lead poisoning: a case-report. J Occup Med Toxicol. 2008;17:23–8.

8. Karimooy HN, Mood MB, Hosseini M, Shadmanfar S. Effects of occupational lead exposure on renal and nervous system of workers of traditional tile factories in Mashhad (northeast of Iran). Toxicol Ind Health. 2010;26:633–8.
9. Karrari P, Mehrpour O, Abdollahi M. A systematic review on status of lead pollution and toxicity in Iran; guidance for preventive measures. DARU J Pharma Sci. 2012;20:2–18.
10. Boon Teh H, Li H, Li SFY. Highly sensitive and selective detection of Pb^{2+} ions using a novel and simple DNAzyme-based quartz crystal microbalance with dissipation biosensor. Analyst. 2014;139:5170–5.
11. Zhang N, Peng H, Wang Sh HB. Fast and selective magnetic solid phase extraction of trace Cd, Mn and Pb in environmental and biological samples and their determination by ICP-MS. Microchim Acta. 2011;17:121–8.
12. Frazzoli C, Bocca B. Validation, uncertainty estimation and application of a sector field ICP MS-based method for As, Cd and Pb in cow's milk and infant formulas. Microchim Acta. 2008;162:43–50.
13. Behbahani M, Abandansari HS, Salarian M, Babapour M, Bagheri A, Nabid MR. Synthesis and application of a thermo sensitive triblock copolymer as an efficient sample treatment technique for preconcentration and ultra-trace detection of lead ions. Microchim Acta. 2014;181:129–37.
14. Liu Y, Liu Z, Wang Y, Dai J, Gao J, Xie J, et al. A surface ion-imprinted mesoporous sorbent for separation and determination of Pb (II) ion by flame atomic absorption spectrometry. Microchim Acta. 2011;172:309–17.
15. Tassali N, Kotera N, Boutin C, Leonce E, Boulard Y, Rousseau B, et al. Smart detection of toxic metal ions, Pb^{2+} and Cd^{2+}, using a Xe-129 NMR-based sensor. Anal Chem. 2014;86:1783–8.
16. Liu SY, Na WD, Pang S, Su XG. Fluorescence detection of Pb^{2+} based on the DNA sequence functionalized CdS quantum dots. Biosens Bioelectron. 2014;58:17–21.
17. Songsungkan J, Chanthai S. Study of allicin extract chelated with some heavy metals (Cu^{2+}, Co^{2+} and Pb^{2+}) by fluorescence quenching method and its antioxidant activity. Asian J Chem. 2014;26:132–6.
18. Liu L, Lin HW. Paper-based colorimetric array test strip for selective and semiquantitative multi-ion analysis: simultaneous detection of Hg^{2+}, Ag^{+}, and Cu^{2+}. Anal Chem. 2014;86:8829–34.
19. Hung YL, Hsiung TM, Chen YY, Huang YF, Huang CC. Colorimetric detection of heavy metal ions using label-free gold nanoparticles and alkanethiols. J Phys Chem C. 2010;114:16329–34.
20. Harrington CF, Clough R, Drennan-Harris LR, Hill SJ, Tyson JF. Atomic spectrometry update. Elemental speciation. J Anal At Spectrom. 2011;26:1561–95.
21. Wang J. Electrochemical nucleic acid biosensors. Anal Chim Acta. 2002;469:63–71.
22. March G, Dung Nguyen T, Piro B. Modified electrodes used for electrochemical detection of metal ions in environmental analysis. Biosensors. 2015;5:241–75.
23. Ebrahimi M, Raoof JB, Ojani R. Novel electrochemical DNA hybridization biosensors for selective determination of silver ions. Talanta. 2015;144:619–26.
24. Ebrahimi M, Raoof JB, Ojani R, Bagheryan Z. A novel electrochemical biosensor for selective determination of mercury ions based on DNA hybridization. Anal Biochem. 2015;488:13–4.
25. Cui L, Wu J, Ju H. Electrochemical sensing of heavy metal ions with inorganic, organic and bio-materials. Biosens Bioelectron. 2015;63:276–86.
26. Li LD, Huang XQ, Guo L. Electrochemical potassium ion sensor based on DNA G-quadruplex conformation and gold nanoparticle amplification. Rare Metals. 2013;32:369–74.
27. Burge S, Parkinson GN, Hazel P, Todd AK, Neidle S. Survey and summary, quadruplex DNA: sequence, topology and structure. Nuc Acids Res. 2006;34:5402–15.
28. Ruttkay-Nedecky B, Kudr J, Nejdl L, Maskova D, Kizek R, Adam V. G-Quadruplexes as sensing probes. Molecules. 2013;18:14760–79.
29. Chiorcea-Paquim AM, Oliveira-Brett AM. Redox behaviour of G-quadruplexes. Electrochim Acta. 2014;126:162–70.
30. Bagheryan Z, Raoof JB, Ojani R, Hamidi-Asl E. Introduction of ketamine as a G-Quadroplex binding ligand using platinum nanoparticle modified carbon paste electrode. Electroanalysis. 2013;25:2659–67.
31. Kong DM, Ma YE, Wu J, Shen HX. Discrimination of G-Quadruplex from duplex and single-stranded DNAs with fluorescence and energy-transfer fluorescence spectra of Crystal Violet. Chemistry. 2009;15:901–9.
32. Bhasikuttan AC, Mohanty J, Pal H. Interaction of malachite green with guanine-rich single-stranded DNA: preferential binding to a G-quadruplex. Angew Chem Int Ed. 2007;46:9305–7.
33. Ge C, Liao J, Yu W, Gu N. Electric potential control of DNA immobilization on gold electrode. Biosens Bioelectron. 2003;18:53–8.
34. Lao R, Song Sh WH, Wang L, Zhang Z, He L, Fan C. Electrochemical interrogation of DNA monolayers on gold surfaces. Anal Chem. 2005;77:6475–80.
35. Lucarelli F, Marrazza G, Turner APF, Mascini M. Carbon and gold electrodes as electrochemical transducers for DNA hybridisation sensors. Biosens Bioelectron. 2004;19:515–30.
36. Wang J, Cai X, Rivas G, Shiraishi H, Farias PAM, Dontha N. DNA electrochemical biosensor for the de-tection of short DNA sequences related to the human immunodeficiency virus. Anal Chem. 1996;68:2629–34.
37. Pournaghi-Azar MH, Hejazia MS, Alipour E. Developing an electrochemical deoxyribonucleic acid (DNA) biosensor on the basis of human interleukine-2 gene using an electroactive label. Anal Chim Acta. 2006;570:144–50.
38. Pang DW, Abruna HD. Micromethod for the investiga-tion of the interactions between DNA and redox-active molecules. Anal Chem. 1998;70:3162–9.
39. Oliveira Brett AM, Macedo TRA, Raimundo D, Marques MH, Serrano SHP. Voltammetric behaviour of mitox-antrone at a DNA-biosensor. Biosens Bioelectron. 1998;13:861–7.
40. Sun X, He P, Liu S, Ye L, Fang Y. Immobilization of single-stranded deoxyribonucleic acid on gold electrode with self-assembled aminoethanethiol monolayer for DNA electro-chemical sensor applications. Talanta. 1998;47:487–95.
41. Cao RG, Zhu B, Li J, Xu D. Oligonucleotides-based biosensors with high sensitivity and selectivity for mercury using electrochemical impedance spectroscopy. Electrochem Commun. 2009;11:1815–8.
42. Livache T, Fouque B, Roget A, Marchand J, Bidan G, Téoule R, et al. Polypyrrole DNA chip on a silicon device: example of hepatitis C virus genotyping. Anal Biochem. 1998;255:188–94.
43. Peng H, Zhang L, Soeller C, Travas-Sejdic J. Conducting polymers for electrochemical DNA sensing. Biomaterials. 2009;30:2132–48.
44. Bonanni A, Pividori MI, Valle MD. Application of the avidin-biotin interaction to immobilize DNA in the development of electrochemical impedance genosensors. Anal Bioanal Chem. 2007;389:851–61.
45. Millan KM, Spurmanis AL, Mikkelsen SK. Covalent immobilization of DNA onto glassy carbon electrodes. Electroanalysis. 1992;4:929–32.
46. Ligaj M, Jasnowska J, Musiał WG, Filipiak M. Covalent attachment of single-stranded DNA to carbon paste electrode modified by activated carboxyl groups. Electrochim Acta. 2006;51:5193–8.

47. Pividori MI, Alegret S. DNA adsorption on carbonaceous materials. Top Curr Chem. 2005;260:1–36.
48. Pividori MI. Merkoc¸i a, Alegret S. DNA immobilization. Electrochemical genosensor design: immobilisation of oligonucleotides onto transducer surfaces and detection methods. Biosens Bioelectron. 2000;15:291–303.
49. Mazloum-Ardakani M, Mandegari AA, Masoum S, Naeimi H. Multiwall carbon nanotubes modified carbon paste electrode for determination of copper(II) by potentiometric and impedimetric methods. JNS. 2012;2:333–43.
50. He P, Xu Y, Fang Y. A review: electrochemical DNA biosensors for sequence recognition. Anal Let. 2005;38:2597–623.
51. Elrouby M. Electrochemical application of carbon nanotube. J Nano Adv Mat. 2013;1:23–38.
52. Reid Bishop G, Chaires JB. Characterization of DNA structures by circular dichroism. Curr Protoc Nucleic Acid Chem. 2002; 7.11.1–7.11.8.
53. Porumb H, Monnot M, Fermandjian S. Circular dichroism signatures of features simultaneously present in structured guanine-rich oligonucleotides: a combined spectroscopic and electrophoretic approach. Electrophoresis. 2002;23:1013–20.
54. Chen J, Zhang J, Zhuang Q, Chen J, Lin X. Electrochemical studies of the interaction of 2-Nitroacridone with DNA and determination of DNA. Electroanalysis. 2007;19:1765–72.
55. Wang Q, Wang X, Yu Z, Yuan X, Jiao K. Spectroscopic and electrochemical studies on the binding mechanism of DNA With An Anthraquinone Biological Dye, Nuclear Fast Red. Int J Electrochem Sci. 2011;6:5470–81.
56. Wang QX, Jiao K, Liu FQ, Yuan XL, Sun W. Spectroscopic, viscositic and electrochemical studies of DNA interaction with a novel mixed-ligand complex of nickel (II) that incorporates 1-methylimidazole and thiocyanate groups. J Biochem Biophys Methods. 2007;70:427–33.
57. Barton JK, Danishefsky AT, Goldberg JM. Tris (phenanthroline) ruthenium(II): stereoselectivity in binding to DNA. J Am Chem Soc. 1984;106:2172–6.
58. Long EC, Barton JK. Demonstrating DNA intercalation. Acc Chem Res. 1990;23:271–3.
59. Ramakrishnan S, Palaniandavar M. Mixed-ligand copper (II) complexes of dipicolylamine and 1, 10-phenanthrolines: the role of diimines in the interaction of the complexes with DNA. J Chem Sci. 2005;117:179–86.
60. Wang XL, Fang JN, Bi YF, Lin HY, Liu GC. Synthesis, DNA-binding, and photocleavage of 2,3-di-2-pyridylquinoxaline-silver(I) complex. Chem Res Chin Univ. 2008;24:15–9.
61. Carter MT, Rodriguez M, Bard AJ. Voltammetric studies of the interaction of metal-chelates with DNA .2. Tris-chelated complexes of cobalt (III) and iron (II) with 1,10-phenanthroline and 2,2′-bipyridine. J Am Chem Soc. 1989;111:8901–11.